Two-Timescale Control of Smart Inverters and

Legacy Devices in Unbalanced Distribution Feeders

Temitayo O. Olowu, *Member, IEEE*, Adedoyin Inaolaji, *Student Member, IEEE*, Sumit Paudyal, *Senior Member, IEEE*, Arif Sarwat, *Senior Member, IEEE*

Abstract—This paper proposes two-time-scale distribution optimal flow (D-OPF) model leveraging legacy grid controllers and smart inverters (SIs) for voltage control on distribution feeders. On the slower time scale, a mixed-integer non-linear programming (MINLP) version of D-OPF provides optimal settings of on-load tap changers (OLTCs), capacitor banks, and SIs' modes and droop settings as per the IEEE-1547. On the fast time scale, using the optimal settings obtained from the first stage of the D-OPF problem, SIs' optimal active/reactive power dispatch problem is solved using a non-linear programming (NLP) model that ensures the active/reactive power setpoints lie on the SIs' droop, ensuring implementation feasibility at the local controller level. The proposed approach is demonstrated using the IEEE-123 unbalanced three-phase test feeder and compared with the case when the use of SI is not prioritized for voltage control. The results show that SIs can be prioritized to enhance the voltage control using optimal mode and droop settings while minimizing the number of operations of legacy grid control devices and optimizing active/reactive power dispatch.

Index Terms—distribution optimal power flow (D-OPF), volt/VAr control (VVC), smart inverter modes and settings, OLTC/VR, and capacitor bank.

I. INTRODUCTION

The use of smart inverters for voltage regulation and control is becoming more attractive with increased DER penetration. According to IEEE-1547 [1], SIs can switch modes of operation. The discrete decision to choose an appropriate SI mode (e.g., constant power factor mode, constant reactive power mode, Volt/VAr mode, Volt/Watt mode) and the piece-wise linear nature of SI droops as prescribed in the IEEE-1547 poses an inherent mathematical challenge in integrating SI constraints into the distribution grid optimal power flow (D-OPF) formulations. Recently, in [2], Volt/VAr and Volt/Watt droop constraints are modeled using a mixed-integer linear programming formulation, and the droop constraints are integrated into a linear-based D-OPF model using first-order voltage approximation methods. Authors of [2-9] consider droop settings as variables in the D-OPF formulation, a significant drawback of these works is that they assume a predefined SI mode selection, which may still lead to sub-optimal solutions since the feeder voltage sensitivities to different SI modes varies due to the variation in X/R values across the feeder [10, 11]. For efficient optimal distribution grid operation, SIs should be coordinated with the existing legacy control devices

This work is supported in part by National Science Foundation grant ECCS-2001732 and CNS-1553494. T. O Olowu, A. Inaolaji, S. Paudyal and A. Sarwat are with the Department of Electrical and Computer Engineering, Florida International University, Miami.

at different time scales to provide efficient volt/var control (VVC). It is, therefore, necessary to configure the D-OPF such that it maximally utilizes SI resources while minimally using legacy devices, as the reduced number of operations of onload tap changers (OLTCs) and capacitor banks (CAPs) will effectively help to reduce the wear and tear of such equipment.

In this context, this paper presents a novel effort to explore multi-mode and multi-droop settings of SIs for coordinated control of SIs and legacy devices at two different timescales. The first stage of D-OPF that determines the SI modes, SI droop settings, CAPs switching status, and OLTC positions is formulated as a mixed-integer non-linear programming (MINLP) problem. The second stage of the D-OPF, formulated as a non-linear programming (NLP) problem, dispatches the active/reactive power setpoints of the SIs on the droops determined from the first stage. The main technical contribution of this work is the formulation of the D-OPF model that sequentially couples the optimization of three voltage control devices (SI modes and settings, CAP, and OLTC/VR). In comparison to the formulation we presented in [12] (where the use of SIs is not prioritized), the SI is given the highest priority in carrying out voltage regulation in order to use most of its available active and reactive power control capabilities. The CAPs status and the OLTC tap position are then optimized respectively afterward. This method is compared with another D-OPF formulation that does not prioritize the use of SIs. The proposed D-OPF approach allows more reactive and active power contribution by the SIs and reduces the number of tap operations by the VRs and CAPs.

The rest of the paper is structured as follows. Section II presents the physics of optimal power flow formulation to be used in the proposed hierarchical control. Section III presents the proposed coordinated and control algorithms. the simulation and results analysis is provided in Section IV. The paper is concluded in Section V.

II. OPTIMAL POWER FLOW FORMULATION

The total voltage deviation, as a result of the voltage control action of the SIs, CAPs, and OLTC/VR, is set as the objective function (OF) as expressed in (1).

$$OF = \min \sum_{i \in \mathcal{N}} \left| \frac{R_i^{eq} \Delta P_i^G + X_i^{eq} \Delta Q_i^G}{v_i} + \frac{1}{v_i} X_i^{eq} \Delta Q_i^c + \Delta Z(tp_i) \cdot I_0 + Z_0 \cdot \Delta I(tp_i) \right|$$
(1)

where \mathcal{N} is the set of all network nodes $i.\ I_0, Y_0, Z_0$ are current injection, admittance, and impedance matrix, respectively, prior to a tap change. $\Delta I(tp_i), \Delta Y(tp_i), \Delta Z(tp_i)$ are the change in current injection, admittance, and impedance matrix after a tap change at node $i.\ R_i^{eq}, X_i^{eq}$ are the equivalent resistance and reactance respectively at the point of interconnection, Q_i^c is the reactive power injection of the capacitor bank, v_i is the instantaneous voltage, and the tp_i is the OLTC/VR tap position. The distribution grid is modeled and set as part of the optimization constraints using the power flow equations in (2)-(6) [13].

$$\Delta P_i(v_i, \delta_i) = P_i^G - P_i^L \quad \forall i \in \mathcal{N}$$
 (2)

$$\Delta Q_i(v_i, \delta_i) = Q_i^G - Q_i^L \quad \forall i \in \mathcal{N}$$
 (3)

where,

$$\Delta Q_i(v_i, \delta_i) = v_i \sum_{k \in N} v_k (\mathcal{G}_{ik} \cos(\delta_{ik}) + \mathcal{B}_{ik} \sin(\delta_{ik})) \quad (4)$$

$$\Delta P_i(v_i, \delta_i) = v_i \sum_{k \in N} v_k (\mathcal{G}_{ik} \sin(\delta_{ik}) - \mathcal{B}_{ik} \cos(\delta_{ik})) \quad (5)$$

The nodal voltage constraint in the network is as expressed in (6).

$$v^{min} \le v_i \le v^{max}, \quad \forall i \in \mathcal{N}$$
 (6)

where P_i^L, Q_i^L are the load active and reactive power, P_i^G and Q_i^G , are active and reactive power injection by PVs, $\mathcal{G}_{ik}, \mathcal{B}_{ik}$ real and imaginary parts of admittance matrix between nodes i and k, while δ_i is the voltage angle. The control of the discrete-control legacy devices makes this formulation MINLP in nature for the first stage of the D-OPF, which requires solving (1) subject to (7). The second stage, on the other hand, does not include dispatching the integer and binary variables of the legacy devices as well as the optimal droop and modes of SIs and can therefore be formulated as an NLP problem, which requires solving (1) subject to (8).

Stage-1:
$$\begin{cases} SIM_{i} \in [m_{1}...m_{5}], & \forall i \in \mathcal{N}_{pv} \\ SIS_{i} \in [V_{i}^{L}...V_{i}^{H}, \phi_{i}], & \forall i \in \mathcal{N}_{pv} \\ tp_{i} \in [-16, ..., +16], & \forall i \in \mathcal{N}_{tp} \\ Q_{i}^{c} = q_{i}^{c} tc_{i}, & \forall i \in \mathcal{N}_{C} \text{ where } tc_{i} \in [0, 1] \end{cases}$$

$$(7)$$

$$\text{Stage-2:} \begin{cases} SIM_{i} = SIM_{i}^{opt} \quad \forall i \in \mathcal{N}_{pv} \\ SIS_{i} = \left[V_{i}^{L} \dots V_{i}^{H}, \phi_{i}\right]^{opt} \quad \forall i \in \mathcal{N}_{pv} \\ tp_{i} = tp_{i}^{opt} \quad \forall i \in \mathcal{N}_{tp} \\ Q_{i}^{c} = q_{i}^{c} tc_{i}^{opt} \quad \forall i \in \mathcal{N}_{C} \\ P_{i}^{min} \leq P_{i}^{G} \leq P_{i}^{pv}, \quad \forall i \in \mathcal{N}_{pv} \\ -Q_{i}^{pv} \leq Q_{i}^{G} \leq Q_{i}^{pv}, \quad \forall i \in \mathcal{N}_{pv} \end{cases}$$

where m is the SI modes, q_i^c reactive power rating of the capacitors, \mathcal{N}_C is the set of nodes with CAPs, \mathcal{N}_{tp} Set of branches with OLTC, SIS and SIS^{opt} are the set of SI setting and optimal setting which contains the optimal breakpoints for the SI droop and the power factor ϕ_i , SIM and SIM^{opt} set of SI modes and optimal modes, P_i^{min} and P_i^{max} are the minimum and maximum available active power from the PV while Q_i^{pv} and P_i^{pv} are the available reactive power generation from the PVs which also depends on the apparent power rating of the SIs.

III. COORDINATION OF LEGACY DEVICES AND SMART INVERTER CONTROL

This paper proposes a two-stage D-OPF for voltage optimization using five SI modes: Volt/Watt, Volt/VAr P-priority, Volt/VAr Q-priority, CPF leading and CPF lagging in coordination with control of OLTC/VRs and CAPs. We propose two coordination methods of the two-stage D-OPF models (depending on whether the algorithm leverages more on SI control than legacy grid devices) called D-OPF-1 and D-OPF-2.

A. D-OPF without SI Priority (D-OPF-1)

In D-OPF-1, the control variables of the first stage D-OPF are the five modes of the SIs, the breakpoints of the SI droop based on the modes, the PF values (for SI CPF mode), the OLTC/VR settings and the CAPs status. Here, the SIs are not emphasized more than legacy grid devices for the control efforts. The algorithm starts by solving a 1-hour resolution D-OPF using the defined first-stage control variables with the objective function defined as expressed in (1). The results of the first-stage $(SIM_i^{opt}, SIS_i^{opt}, tc_i^{opt})$ and tp_i^{opt} are passed on to the second stage D-OPF. The second stage D-OPF is solved using the values of SIM_i^{opt} , SIS_i^{opt} , tc_i^{opt} and tp_i^{opt} with the active power and reactive power setpoint of SIs as the optimization control variables at a 1-minute resolution. Using the hourly optimal values for the first-stage D-OPF, the second stage is solved 60 times, after which the first-stage D-OPF is solved again for the next hour. The pseudo-code for the proposed D-OPF-1 is presented in Algorithm 1.

Algorithm 1: without SI Priority (D-OPF-1)

```
1: procedure SOLVE FOR SIM_i^{opt}, SIS_i^{opt}, tp_i^{opt}, tc_i^{opt}, Q_{i,t}^G, P_{i,t}^G \forall i \in
      \mathcal{N}_{pv}, \mathcal{N}_{C}, \mathcal{N}_{tp}
            Begin time T=1
 2:
 3:
            Begin time t=1
                                                                      \begin{array}{c|c} \rhd \text{ Solve 1-hr D-OPF} \\ \rhd SIM_{i,T}^{opt}, SIS_{i,T}^{opt}, tp_{i,T}^{opt}, tc_{i,T}^{opt} \\ \rhd \text{ Solve 1-min D-OPF} \\ \rhd \text{ Solve } Q_i^G, P_i^G \end{array} 
 4:
            while T \le 24 do
                   Solve (1) s.t. (7)
 6:
                   while t \le 60 \times t do
 7:
                        Solve (1) s.t. (8)
 8:
                        if t = T \times 60 then
 9.
                               T=T+1
10:
                               Execute step 4
                         else
11:
12:
13:
                               Execute step 6
14:
                        end if
                   end while
16:
             end while
17: end procedure
```

B. D-OPF with SI Priority (D-OPF-2)

In order to reduce the number of D-OPF-1 control variables solved at one go (to improve computational efficiency, minimize operations of legacy grid devices, and emphasize SI control over the legacy grid devices) in the first stage D-OPF, the D-OPF-2 control variables are solved sequentially. In this approach, the optimal modes and settings of the SI are of the highest priority. Within the stage-1 of D-OPF-2, a first D-OPF is solved which determines SIM_i^{opt} and SIS_i^{opt} .

This is done to allow the SI to actively carry out the voltage regulation to its maximum capacity. Afterward, the values of SIM_i^{opt} and SIS_i^{opt} are passed to the second D-OPF problem in stage 1, while the CAPs status tc_i is set as the optimization control variable. The value of the newest voltage deviation objective is computed and compared to the voltage deviation objective obtained from the first D-OPF solution. If the latter is lesser, the new optimal values of tc_i^{opt} are saved, and if otherwise, CAPs status tc_i^{opt} is reverted to its previous status. Then, the values of SIM_i^{opt} , SIS_i^{opt} , and tc_i^{opt} are passed to the third D-OPF problem in stage 1 while the tap position tp_i is set as the control variable. The value of the newest voltage deviation objective is computed and compared to the voltage deviation objective obtained from the updated second D-OPF. If the latter is lesser, the new optimal values of tp_i^{opt} are saved, and if otherwise, the tap position tp_i^{opt} is reverted to its previous tap position. The updated objective function is set as the lower value. The updated values of SIM_i^{opt} , SIS_i^{opt} , tc_i^{opt} and tp_i^{opt} are passed to the stage-2 of D-OPF-2. As described in the previous D-OPF-1 algorithm, a highresolution D-OPF (1-minute) is solved to optimally dispatch the active and reactive power of the PVs. The Pseudo-code of the proposed D-OPF-2 is presented in Algorithm 2.

Algorithm 2: with SI Priority (D-OPF-2)

```
1: procedure Solve for SIM_i^{opt}, SIS_i^{opt}, tp_i^{opt}, tc_i^{opt}, Q_{i,t}^G, P_{i,t}^G \forall i \in
      \mathcal{N}_{pv}, \mathcal{N}_{C}, \mathcal{N}_{tp}
            Begin time T=1
 3:
            Begin time t=1
 4:
            while T \le 24 do
                                                                                        ⊳ Solve 1-hr D-OPF
                                                                              \triangleright OF^1, SIM_{i,T}^{opt}, SIS_{i,T}^{opt} \triangleright OF^2, tc_{i,T}^{opt}
 5:
                  Solve (1) s.t. (7)
 6:
                  Solve (1) s.t. (7)
                  \delta v = OF^1 - OF^2
 7:
                  if \delta v > 0 then
 8:
                       tc_{i,T}^{opt} = tc_{i,T}^{opt}
 9:
                        OF = OF^2
10:
11:
                                 =tc_{:\,\, ^{\prime }}^{opt}
12:
                       OF = OF^{1}
13:
14:
                                                                                                   \triangleright OF^3, tp_{i,T}^{opt}
15:
                  Solve (1) s.t. (7)
                  \delta v = OF - OF^3
16:
                  \begin{array}{c} \text{if } \delta v > 0 \text{ then} \\ tp_{i,T}^{opt} = tp_{i,T}^{opt} \end{array}
17:
18:
                        OF = OF^3
19:
20:
                        tp_i^{opt} = tp_i^{opt, T-1}
21:
                        OF = OF
22:
                                                                   \begin{array}{c} \rhd SIM_{i,T}^{opt}, SIS_{i,T}^{opt}, tp_{i,T}^{opt}, tc_{i,T}^{opt} \\ \rhd \text{ Solve 1-min D-OPF} \end{array}
23:
                  end if
                  while t \le 60 \times t do
24:
                                                                                              \triangleright \ \text{Solve} \ Q_i^G, P_i^G
25:
                        Solve (1) & (8)
26:
                       if t = T \times 60 then
27:
                              T=T+1
28:
                              Execute step 4
29.
                        else
30:
31:
                              Execute step 25
32:
                       end if
                  end while
            end while
34:
35: end procedure
```

IV. SIMULATION RESULTS AND ANALYSIS

In order to validate and compare the D-OPF-1 and D-OPF-2 models, the IEEE 123-node system, as shown in Fig. 1, is

used. The IEEE 123-node test feeder has a nominal voltage

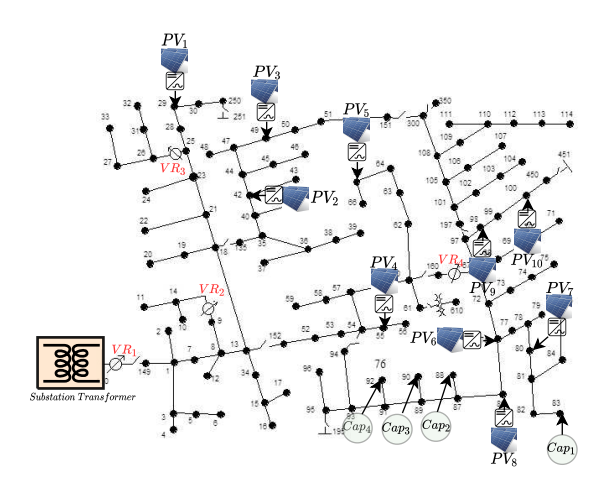


Fig. 1: IEEE 123 test node system with ten PVs integrated.

of 4.16 kV with four voltage regulators (VR₁, VR₂ VR₃, and VR₄) and four CAPs (Cap₁, Cap₂, Cap₃, and Cap₄). The CAPs include one 600 kVAr three-phase and three 50 kVAr single-phase. Ten units of PV systems rated 100 kW are integrated into the feeder. The PV's SIs were sized at 125% of the maximum DC capacity of the PVs. For the Volt/VAr (P-priority), the maximum $Q_i^G = \frac{\sqrt{1.25^2 - 1^2}}{1.25} = 0.6$ [14] while for the Volt/VAR (Q-priority), the maximum $Q_i^G \leq S_i^{SI}$ [15]. It is worthy of note that in the Volt/VAR (Q-priority) mode, the SI is allowed to curtail the active power as much as required by the setting $Q_i^G \leq S_i^{SI}$. Each SIs is allowed to take five modes (set as variables in stage-1), which include: Volt/Watt, Volt/VAr P-priority, Volt/VAr Q-priority, and constant power factor (CPF: leading and lagging). The simulation is done for cloudy day PV generation. An hourly sampled PV generation profile is used to dispatch the optimal VR, CAPs status, and SI modes and settings while the 1-minute resolution PV generation profile is used for the dispatch of the SI's active and reactive power.

A. Optimal SI Modes and Settings

The optimal SI modes and settings for stage-one of D-OPF-1 and D-OPF-2 are as shown in Figs. 2a, 2b respectively. The modes and SI settings are plotted for the periods of PV power generation between 8 am to 4 pm. As seen in Fig. 2a and 2b, the algorithm effectively selects the optimal modes of the SIs for each hour. All the possible SI modes (Volt/Watt, Volt/VAr (P-priority), Volt/VAr (Q-priority), CPF (leading and lagging)) considered during the optimization are used by the SIs for effective voltage regulation. The summary of the number of times optimal SI modes are changed is presented in Table I.

TABLE I: Number of SI Modes using D-OPF-1 vs D-OPF-2 (Hour 8-16)

SI Modes	D-OPF-1	D-OPF-2
CPF (Leading & Lagging)	38	29
Volt/Watt	9	21
Volt/VAr (P-Priority)	13	4
Volt/VAr (Q-Priority)	30	36

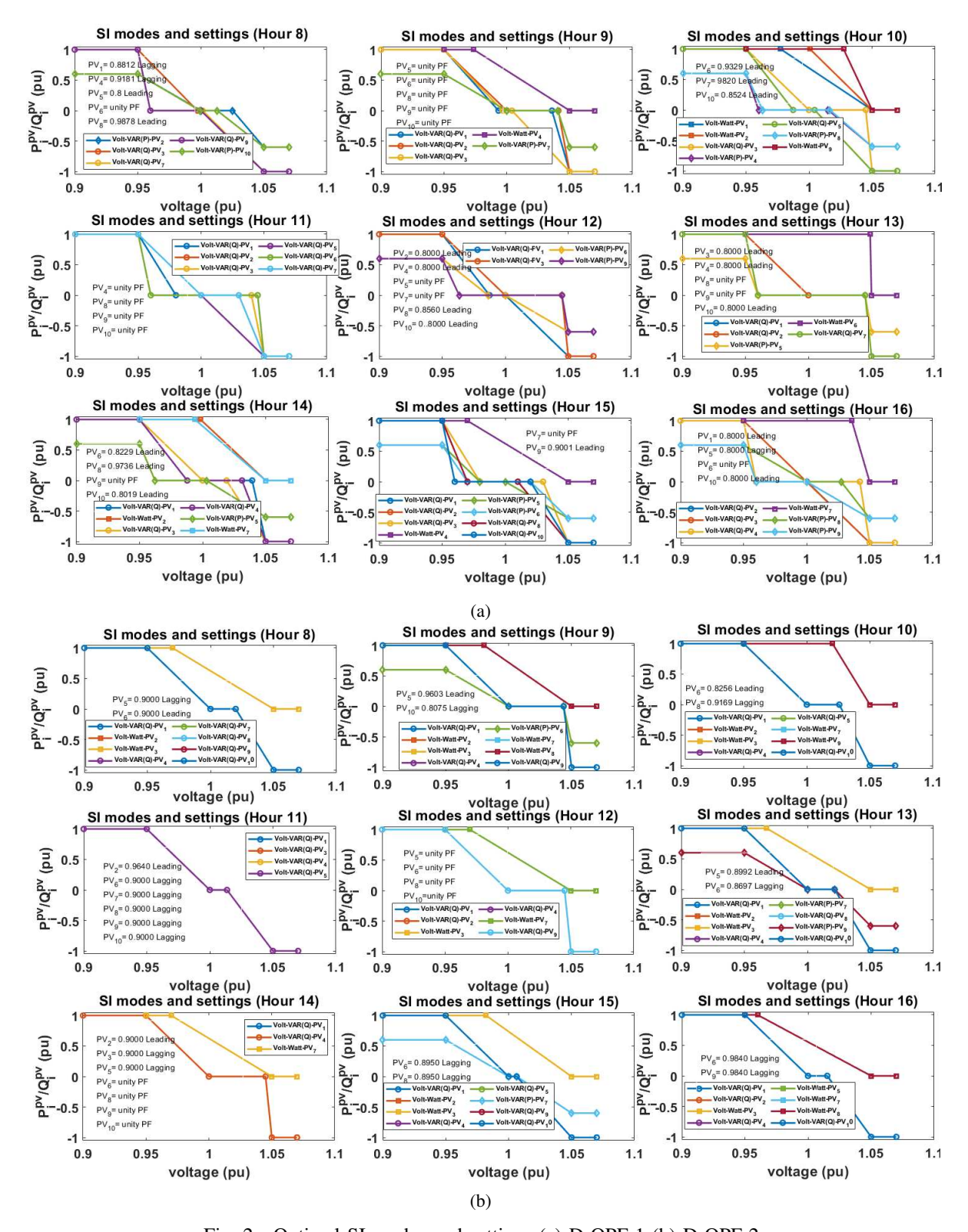


Fig. 2: Optimal SI modes and settings (a) D-OPF-1 (b) D-OPF-2.

B. Optimal Tap Positions and CAPs Status

The optimal tap positions using the proposed D-OPF-1 and D-OPF-2 algorithms for VR_1 , VR_2 , VR_3 , and VR_4 is as shown in Fig. 3. Due to the hierarchy of operations introduced in the D-OPF-2 algorithm, the number of tap operations is reduced.

The summary of the tap changes for the four voltage regulated is tabulated in Table II. The total tap changes with the D-OPF-1 is 230, while that of D-OPF-2 is 165. This shows \approx 28% reduction in the tap operation with the use of D-OPF-2 compared to that of the D-OPF-1. Table III also shows \approx

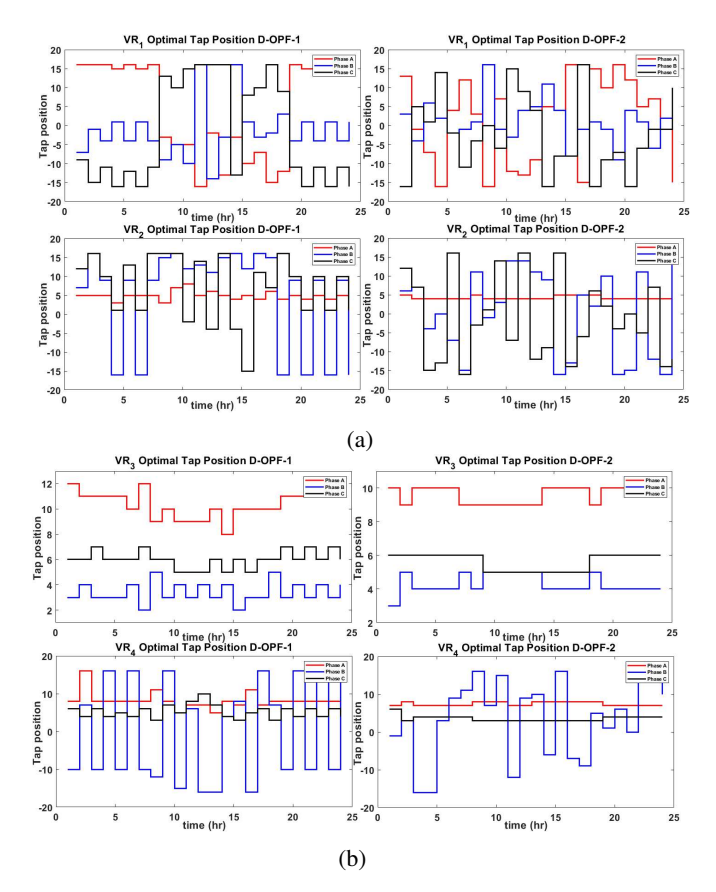


Fig. 3: Optimal tap positions (using D-OPF-1 and D-OPF-2) for (a) VR_1 & VR_2 (b) VR_3 & VR_4 .

TABLE II: Tap changes D-OPF-1 and D-OPF-2

	D-OPF-1			D-OPF-2		
	Ph A	Ph B	Ph C	Ph A	Ph B	Ph C
VR ₁	20	23	21	23	23	21
VR_2	19	23	21	5	22	23
VR ₃	10	20	16	6	8	2
VR_4	12	22	23	6	22	4
Total	230			165		

17% increase in CAPs utilization with the use of D-OPF-2 compared to that of the D-OPF-1.

TABLE III: CAPs status for D-OPF-1 and D-OPF-2

	Cap ₁ ,Cap ₂ ,Cap ₃ and Cap ₄ , $\sum_{1}^{24} tc_{i,T}^{opt}$		
	D-OPF-1	D-OPF-2	
ON	76	92	
OFF	20	4	

C. Active and Reactive Power Dispatch

Using the values of SIM_i^{opt} , SIS_i^{opt} , tc_i^{opt} and tp_i^{opt} , the second-stage D-OPF for one-minute resolution is solved to determine Q_i^G, P_i^G . The sum of all P-Q dispatch by all the SIs on a cloudy day considered is as shown in Fig. 4. The negative values of Q_i^G (on the Q (kVAr) plot) represent the reactive power absorption, while the positive values represent the reactive power injection. The active power curtailment for

both algorithms is also shown in Fig. 5. It can be seen from the active power dispatch that both algorithms curtail the active power at some intervals and inject/absorb reactive power for effective voltage regulation. Within the time period considered, the D-OPF-1 curtails total energy of 80.7 kWhr. Also, the D-OPF-2 curtails total energy of 221.5 kWhr. The active power curtailment by both algorithms is determined based on the optimal SI modes and settings. The use of the Volt/VAr (P-priority) by both algorithms allows the SIs to curtail the active power generation for effective voltage regulation.

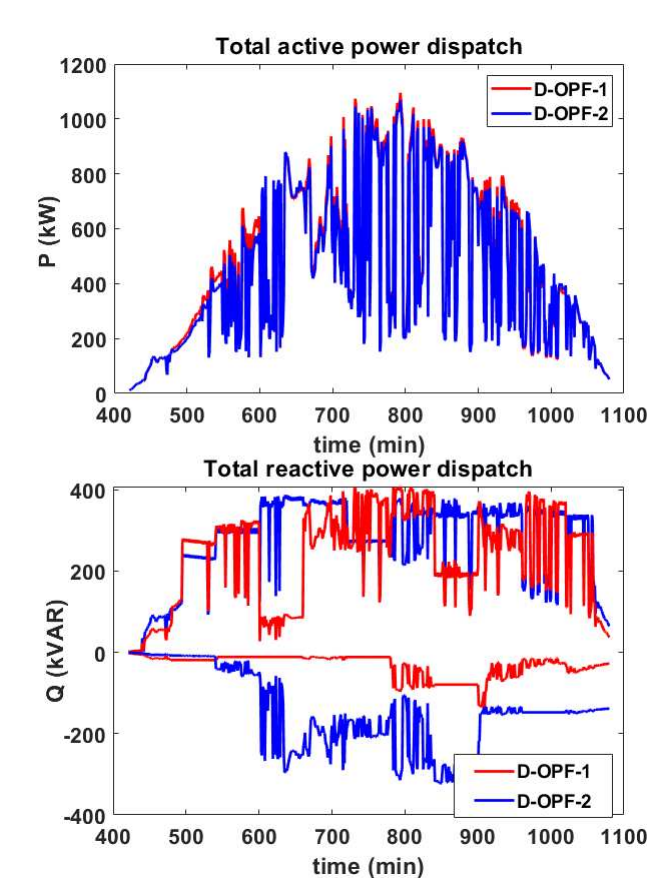


Fig. 4: Active-Reactive Power dispatch.

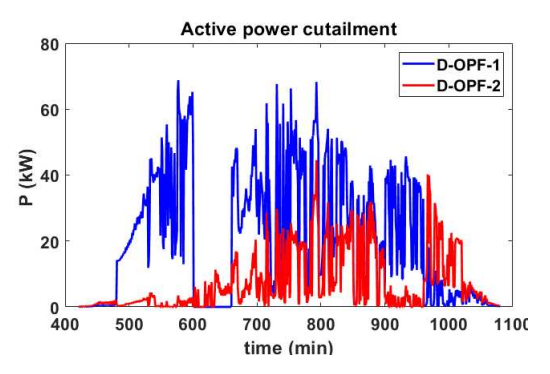


Fig. 5: Active power curtailment.

Also, both algorithms inject/absorb their optimal reactive power based on the SI modes and settings. From the reactive power dispatch plot (Fig. 4, more reactive power is either absorbed/injected using D-OPF-2 to control the feeder voltage compared to that of D-OPF-1.

D. Voltage variance analysis

The phase voltage profiles of all the PV using the proposed D-OPF-1 and D-OPF-2 are extracted, and their variance is computed. The results are as shown in Fig. 6. The variance

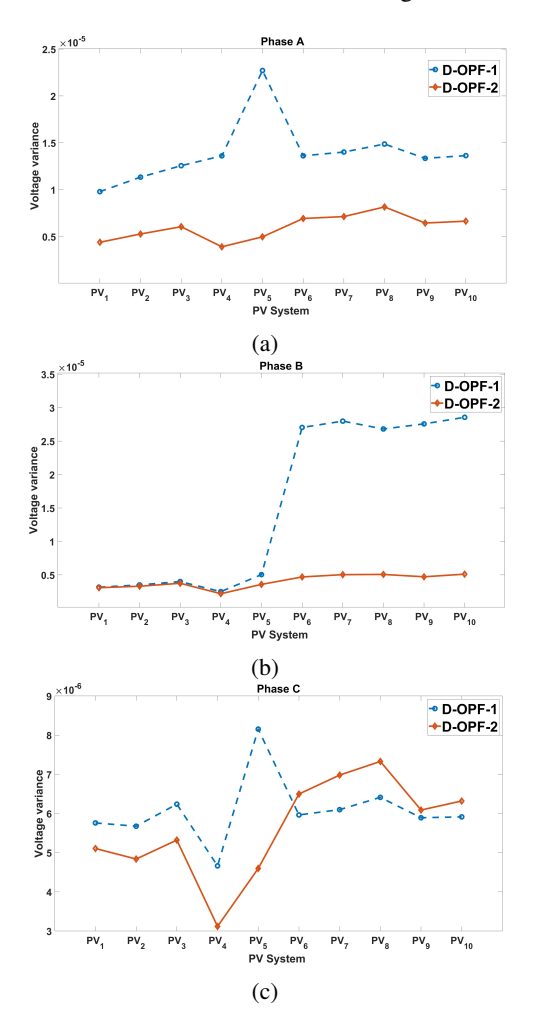


Fig. 6: Variance of the phase voltages of each PV.

values indicate the measure of the variability (dispersion) of each phase voltage of each PV system. Comparing the voltage variance values of D-OPF-1 and D-OPF-2, D-OPF-2 has a lower voltage variation on most of the PVs compared to D-OPF-1 due to the priority given to the SIs. These results show the benefits of prioritizing the use of SIs and optimally selecting the modes and the droop settings of the SIs for effective voltage control.

V. CONCLUSION AND FUTURE WORK

This paper presented a distribution-grid optimal power flow (D-OPF) framework to optimally dispatch the mode (Volt/Watt, Volt/VAr P-priority, Volt/VAr Q-priority, constant power factor) and droop settings of smart inverters (SIs) as per the IEEE-1547. Since the SIs are capable of operating at a fast time scale, the problem is decoupled into two time-scale

problems to coordinate the dispatch of legacy grid controller, SIs' droops and mode selections, and SIs' active/reactive power setpoints. We presented two D-OPF formulations, one in which the use of SIs is not prioritized (D-OPF-1) and the second version of D-OPF, which attributes the highest priority of voltage control to the SI. The proposed formulation and algorithms are tested on the standard IEEE 123 test feeder. The results show (in comparison with other SI modes and droop selection methods in literature) the effectiveness and feasibility of proposed algorithms in optimally setting the droop and mode of SIs in coordination with legacy grid control devices for optimal VVC performance. Also, assigning higher voltage control priority to SIs shows that more effective voltage control and regulation can be achieved.

REFERENCES

- D. G. Photovoltaics and E. Storage, "IEEE standard for interconnection and interoperability of distributed energy resources with associated electric power systems interfaces," *IEEE Std*, pp. 1547–2018, 2018.
- [2] A. Inaolaji, A. Savasci, and S. Paudyal, "Distribution grid optimal power flow in unbalanced multi-phase networks with volt-var and voltwatt droop settings of smart inverters," *IEEE Transactions on Industry Applications*, 2022.
- [3] P. Lusis, L. L. Andrew, A. Liebman, and G. Tack, "Interaction Between Coordinated and Droop Control PV Inverters," in *Proc. Eleventh ACM International Conference on Future Energy Systems*, 2020, pp. 314–324.
- [4] A. Savasci, A. Inaolaji, and S. Paudyal, "Two-stage volt-var optimization of distribution grids with smart inverters and legacy devices," *IEEE Transactions on Industry Applications*, vol. 58, no. 5, pp. 5711–5723, 2022.
- [5] T. Gush, C.-H. Kim, S. Admasie, J.-S. Kim, and J.-S. Song, "Optimal Smart Inverter Control for PV and BESS to Improve PV Hosting Capacity of Distribution Networks Using Slime Mould Algorithm." *IEEE Access*, vol. 9, pp. 52 164–52 176, 2021.
- [6] T. O. Olowu, A. Inaolaji, A. Sarwat, and S. Paudyal, "Optimal volt-var and volt-watt droop settings of smart inverters," in 2021 IEEE Green Technologies Conference (GreenTech), 2021, pp. 89–96.
- [7] V. T. Dao, H. Ishii, and Y. Hayashi, "Optimal parameters of volt-var functions for photovoltaic smart inverters in distribution networks," *IEEJ Transactions on Electrical and Electronic Engineering*, vol. 14, no. 1, pp. 75–84, 2019.
- [8] A. Inaolaji, A. Savasci, and S. Paudyal, "Optimal Droop Settings of Smart Inverters," in *Proc. 48th Photovoltaic Specialists Conference* (PVSC). IEEE, 2021, pp. 2584–2589.
- [9] I. Murzakhanov, S. Gupta, S. Chatzivasileiadis, and V. Kekatos, "Optimal design of volt/var control rules for inverter-interfaced distributed energy resources," arXiv preprint arXiv:2210.12805, 2022.
- [10] M. Rylander, M. J. Reno, J. E. Quiroz, F. Ding, H. Li, R. J. Broderick, B. Mather, and J. Smith, "Methods to determine recommended feeder-wide advanced inverter settings for improving distribution system performance," in *Proc. IEEE 43rd Photovoltaic Specialists Conference (PVSC)*, 2016, pp. 1393–1398.
- [11] H. Li, M. Rylander, and J. Smith, "Analysis to inform CA grid integration: Methods and default settings to effectively use advanced inverter functions in the distribution system," EPRI, Palo Alto, CA, 2015.
- [12] T. Olowu, A. Inaolaji, S. Paudyal, and A. Sarwat, "Optimal mode and droop setting of smart inverters," in *Proc. Power & Energy Society General Meeting (PESGM)*. IEEE, 2023, pp. 1–5.
- [13] Z. Yang, H. Zhong, A. Bose, Q. Xia, and C. Kang, "Optimal power flow in ac-dc grids with discrete control devices," *IEEE Transactions* on *Power Systems*, vol. 33, no. 2, pp. 1461–1472, 2018.
- [14] R. A. Jabr, "Robust volt/var control with photovoltaics," *IEEE Transactions on Power Systems*, vol. 34, no. 3, pp. 2401–2408, 2019.
- [15] J. Seuss, M. J. Reno, R. J. Broderick, and S. Grijalva, "Analysis of PV advanced inverter functions and setpoints under time series simulation," *Sandia National Laboratories SAND2016-4856*, 2016.